JOURNAL OF THERMOPHYSICS AND HEAT TRANSFER
Vol. 23, No. 1, January–March 2009

Boiling at Subatmospheric Pressures with Enhanced Structures

Aniruddha Pal*
Applied Materials, Inc., Sunnyvale, California 94086
and
Yogendra Joshi†
Georgia Institute of Technology, Atlanta, Georgia 30332

DOI: 10.2514/1.31416

Experiments were performed to study the effects of subatmospheric pressures on the boiling of water from enhanced structures. The experiments were conducted at 9.7, 15, and 21 kPa. The boiling enhancement structure was integrated within the evaporator of a compact thermosyphon and had stacked-layer geometry. Each layer of the porous structure had dimensions of 12.7 × 12.7 × 1 mm (length × breadth × thickness). Four different geometries of the structure were used, each having 1 layer, 2 layers, 4 layers, and 6 layers, respectively. The boiling curves from the enhancement structures were compared with subatmospheric pressure boiling from a plain surface. Subatmospheric pressure boiling achieved heat fluxes in excess of 100 W/cm^2 with negligible incipient superheat, while keeping boiling surface temperatures below 85°C. Reduced pressures also resulted in reduction of the heat transfer coefficient with a decrease in saturation pressure. The boiling enhancement structure showed considerable heat transfer enhancement compared with boiling from a plain surface and also increased the critical heat flux limit. Increased height of the structure decreased the heat transfer coefficient and suggested the existence of an optimum structure height for a particular saturation pressure.

Nomenclature

A	=	external surface area of heater, m^2
h	=	heat transfer coefficient, W/m$^2 \cdot$ K
k	=	thermal conductivity, W/m $\cdot$ K
Q	=	heat input, W
q''	=	heat flux, W/cm^2
T	=	temperature, °C
ΔT	=	wall superheat, $T_w - T_{\text{sat}}$, °C
ϕ	=	diameter, mm

Subscripts

c	=	copper
h	=	heater
s	=	exposed surface
sat	=	saturation condition
w	=	wall

I. Introduction

ONE of the most efficient ways of employing liquid cooling of microelectronics is through successive evaporation and condensation of the working fluid in a two-phase thermosyphon loop, which consists of the evaporator and the condenser chambers connected to each other in a closed loop. Heat is transferred from the source to the evaporator often through an interface, vaporizing the working fluid in the evaporator. The vapor is driven to the condenser due to buoyancy. The condensed liquid returns to the evaporator through the connecting tube. With the condenser placed above the evaporator, the buoyant pressure head generated due to the difference in density between the liquid-rich and the vapor-rich tubes drives the flow through the loop; as such, no external driving force is required.

Received 4 April 2007; revision received 14 January 2008; accepted for publication 2 March 2008.

*Mechanical Engineer, Etch Products Business Group.
†Professor, G. W. Woodruff School of Mechanical Engineering.

Previous research [1–11] has shown the prospect of a thermosyphon as a compact, high-performance thermal management device, both in terms of flexibility afforded through the independent placement of the evaporator and the condenser, and the cooling capacity range. Recently, Pal et al. [12] demonstrated an implementation of a thermosyphon in a commercial desktop computer using water as the working fluid and incorporating boiling enhancement structure in the evaporator. Their study showed that water at reduced pressures performed as a better working fluid than PF5060, a dielectric liquid. Reduced pressures lower the saturation temperature, resulting in boiling initiation at lower temperatures, necessary for electronic cooling applications. Apart from that, the use of boiling enhancement structures has been shown to aid in bubble nucleation during boiling, reduce incipience excursion, and also induce a considerable size reduction of the evaporator. However, detailed studies on the boiling of water at subatmospheric pressures with enhancement structures are absent, and the operational characteristics of thermosyphon at reduced pressures are poorly understood.

A. Boiling at Subatmospheric Pressures

Boiling of water at subatmospheric pressures has been done mostly on plain surfaces or wires and, in some cases, on machine roughened surfaces. One of the early works on boiling at subatmospheric pressures was by Van Stralen [13], who studied boiling of water and a mixture of methylethylketone on an electrically heated platinum wire within a pressure range of 13–101-kPa. A decrease in pressure delayed the onset of nucleate boiling and led to increase in the bubble sizes, while reducing the maximum heat flux attained. Ponter and Haigh [14] visualized boiling of water for the pressure range of 13–101 kPa with a tubular stainless steel heater in a stainless steel cylinder. Similar to Van Stralen [13], they also observed a reduction in potentially active bubble nucleation sites. Further, they also observed that the increase in pressure led to an increase in the critical heat flux. Another notable study on the mechanism of nucleate boiling at atmospheric and subatmospheric pressures was by Miyauchi and Yokura [15], who suggested that a rapidly growing bubble would accelerate the liquid surrounding the bubble, which will increase the pressure inside the bubble with respect to the outside pressure. They believed that the process would induce a higher saturation pressure inside the bubble, leading to a higher wall superheat, which will suppress the bubble growth rate.

Later, Van Stralen et al. [16] experimentally investigated the growth rate of vapor bubbles in water using a nickel-plated copper heating surface for a pressure range of 2–26.7 kPa. They observed that the bubble departure time and departure radius increased substantially with a decrease in operating pressure.

Joudi and James [17] focused on a pressure range of 25–101.3 kPa for boiling in water, R-113, and methanol and observed fluctuations in the surface temperature during incipience. They noted that decreasing pressure lowered the incipient superheat. Fath and Judd [18] investigated microlayer evaporation and found higher wall superheats with a decrease in operating pressure. With an increase in surface heat flux, they found an increase in the bubble generation site density, which facilitated the transfer of additional heat. Tewary et al. [19] observed that the heat transfer coefficient decreases with a decrease in saturation pressure in the nucleate boiling regime within a pressure range of 60–100 kPa. They studied nucleate boiling on a horizontal tube at atmospheric and subatmospheric pressure with water and NaCl solution. McGillis et al. [20] investigated the boiling of water in a thermosyphon configuration at subatmospheric pressures using a plain surface with surface enhancements. They observed that lower pressure generated larger nucleation bubbles, which impeded the growth of active nucleation sites, resulting in larger wall superheats. However, surface enhancements improved the heat transfer with lower wall superheat and increased the critical heat flux. More recently, Rainey et al. [21] did experiments with FC-72 at reduced pressures from microporous structures in the pressure range of 30–150 kPa for a liquid subcooling range of 0–50°C and observed that an increase in pressure brings an increase in critical heat flux (CHF) with a decrease in boiling incipience.

B. Boiling with Enhancement Structures

The high heat flux capability of enhanced structures for boiling with dielectric liquids and refrigerants makes them excellent candidates for integrating in the evaporator of compact thermosyphons. However, the heat flux capability of enhanced structures for boiling with water is not fully understood. Existing literature on boiling with enhancement structures shows that the enhancement varied from machine-induced roughness to a more complex structure of interconnected pores and channels. Most of these studies were done at atmospheric pressure. Nakayama et al. [22] studied boiling from enhanced structures at atmospheric pressures with R-11, water, and liquid nitrogen. The boiling enhancement structure was made of interconnected internal cavities in the form of tunnels and small pores, connecting the pool liquid and the tunnels. They did their experiments at decreasing heat fluxes and found that hysteretic behavior was less pronounced than that observed in boiling from plain surfaces. For enhanced surfaces, the wall superheat remained much lower than for plain surfaces for the range of heat flux applied for the experiments. Bergles and Chyu [23] investigated pool boiling of water and R-113 from surfaces with porous metallic coatings. Their observations revealed hysteresis in the boiling process; however, surface enhancements improved the heat transfer. Experiments on boiling with commercial enhanced surfaces, Gewa-T and Thermoexcel-E, were done by Marto and Lepere [24]. The enhanced surfaces always produced higher heat transfer coefficients than plain surfaces, though they noticed some variation in the level of the performance among the various surfaces at low and high heat fluxes. Later, Nakayama et al. [25] experimented on the enhancement of boiling heat transfer using a stud, which has fine surface structures and was attached to the back of the heat-dissipating device. Their experiments were done at atmospheric pressure with both flourinert (FC-72) and refrigerant (R-11). They observed that the boiling curve has a steeper slope before established nucleation than is expected in natural convection. Anderson and Mudawar [26] used FC-72 as a working fluid and found that boiling incipience increased with more nonboiling time (idle time between successive boiling experiments). They found that their micro-structures significantly shifted the boiling curves toward lower superheats, while increasing the incipience excursion. However, increasing roughness of the boiling surface initiated incipience earlier and reduced the excursion.

The previous studies on enhanced structures were mainly performed at atmospheric pressures, however, the effect of subatmospheric pressures on enhanced structures is not properly understood. Moreover, there is also a lack of understanding on the effects of enhanced structure and subatmospheric pressures in a compact system like a dual-chamber thermosyphon. The current study explores the results of a recent investigation of Pal and Joshi [27] and performs a comprehensive characterization of the boiling of water at reduced pressures in a compact thermosyphon loop using boiling enhancement structures and compares the results with existing correlations and previous observations. The thermal performance of a thermosyphon using water as a working fluid is explored experimentally for various system pressures, enhancement structure geometries, and external heat loads. The performance of the system is also compared with boiling from a plain surface.

II. Experimental Apparatus

The test setup (similar to Pal and Joshi [27]), seen in Fig. 1, consisted of the evaporator and the condenser connected through flexible copper tubing (external diameter 6.35 mm). This arrangement created a thermosyphon loop with the condenser placed at a higher elevation than the evaporator, which helped in gravity-assisted draining of the condensed liquid from the condenser to the evaporator. The experimental setup was designed to monitor and control the various process parameters through a data acquisition system.

A detailed sketch of the evaporator along with the heat-generating unit is shown in Fig. 2. The evaporator was an annular cylindrical chamber, 65 mm in height (height of the cavity inside was ~42 mm) and a 38 mm inner diameter, made of translucent polycarbonate, which allowed the viewing of the liquid level inside the chamber and the initiation of bubble generation. The top and bottom of the evaporator chamber were enclosed by two polycarbonate caps, each one press-fitted with two Buna-N O-rings. The top cap allowed the passing of the vapor to the condenser, while the bottom cap was press-fitted to the heat input block and allowed the introduction of the enhancement structure into the evaporator chamber. The heat input block was a cylindrical copper rod, 20 mm in diameter and 82 mm in length, press-fitted to the bottom cap with double O-rings. One end of the block was machined to a 12.7 mm square cross section of around 2 mm in height. After fitting the copper rod in the bottom cap (through a square shaped hole ~12.7 mm), the square surface was flush with the top surface of the bottom cap. The exposed square

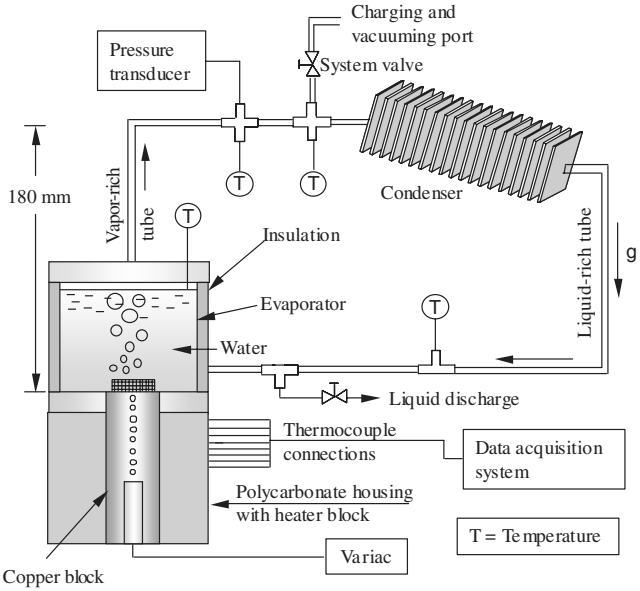

Fig. 1 Schematic of the experimental setup.

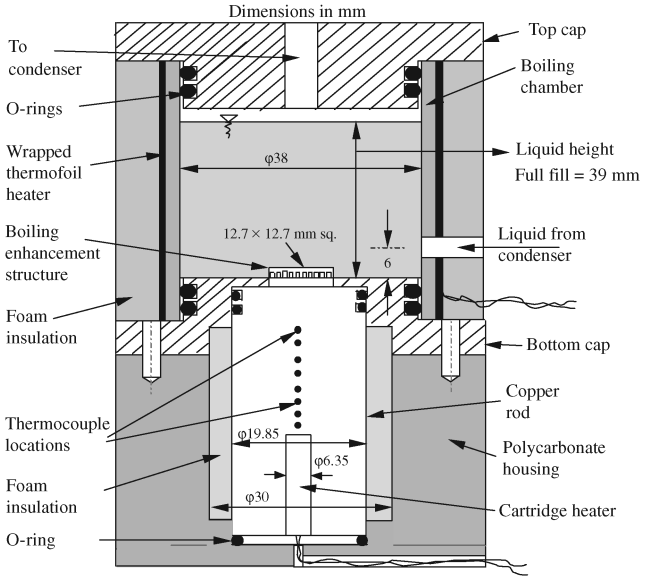

Fig. 2 Detailed sketch of the evaporator assembly.

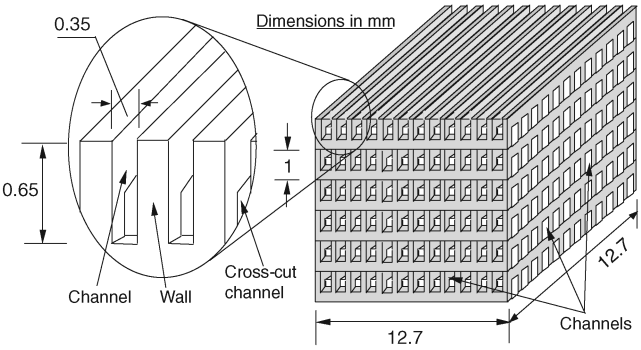

Fig. 3 Detailed sketch of the enhanced structure with stacked multiple layers (six layers shown).

surface was used as the boiling surface in the baseline study. Boiling enhancement structures were soldered to the square surface for the rest of the experiments. The other end of the block had a drilled hole for accommodating the heat source. A cartridge heater (maximum power of 200 W) was used as the heat source. A high-temperature-resistant (up to 200°C) and high-thermal-conductivity paste ($k = 2.3$ W/m · k) was used between the cartridge heater surface and the drilled-hole surface to reduce thermal contact resistance between them.

For the present study, deionized water was chosen as the working fluid, and for all the experimental runs the evaporator was charged almost to its full capacity with approximately 0.06 kg of water. The power to the cartridge heater was supplied from a variac (0–140 V), connected in series to a 1 Ω precision resistor. The voltage drops across the cartridge heater and the precision resistor were measured separately to obtain the power input to the heater. Temperatures at various points in the system were measured with type T (copper-constantan) sheathed thermocouples (diameter ∼0.08 mm). The temperature gradient along the copper block was calculated from the temperatures measured by eight thermocouples, which were fitted inside small grooves along the length of the copper block at varying distances from the boiling surface. Grounded type T thermocouple probes were placed at the following points inside the system: the evaporator chamber, in the flow path between the evaporator and the condenser, the condenser entry, and the condenser exit. The pressure inside the system was measured by a high precision current output (4–20 mA) pressure transducer (0–200 kPa absolute), which was accurate up to 0.13% of the full scale.

A principal focus of the study was to investigate the effect of enhancement structure on boiling at subatmospheric pressures. The structure used in the present study is similar in construction to those used by Nakayama et al. [25], Ramaswamy et al. [28], Launay et al. [29], and Pal and Joshi [27]. A detailed sketch of the enhancement structure used in the present study is shown in Fig. 3. The basic component of the structure was a single layer of copper ($12.7 \times 12.7 \times 1$ mm), in which an array of rectangular channels (0.35 mm wide) was cut in mutually perpendicular directions on both sides. The depth of each channel is more than half the thickness of the copper layer, resulting in the intersection of channels from both sides, forming an array of square pores.

The copper structure layers were fabricated using the wire electrodischarge machining (EDM) method. The individual copper layers were stacked on the square surface of the copper block with a layer of 63Pb-37Sn ribbon solder in between them. The stacked structure was bonded to the copper block by achieving a junction temperature greater than 200°C. The enhancement structure formed (Fig. 3), resulted in geometrical features that are different from the geometries of surface enhancements used in previous studies on subatmospheric pressure boiling. For the present study, four different geometries of the structure were considered: 1 layer, 2 layers, 4 layers, and 6 layers.

III. Experimental Procedure

Leakage testing (allowable leakage ∼0.1–0.2 kPa/day) was done by evacuating the thermosyphon to 2 kPa and leaving the setup at idle conditions at room temperature for a 24 h period. Every experimental run was preceded by a degassing operation of the working fluid in a separate setup. The evaporator chamber for the degassing operation was connected to a spiral tube reflux condenser through a quick coupling (valved) connection. Vigorous boiling was continued in the degassing chamber for an hour, and then the liquid was allowed to reach room temperature. After the degassing procedure, the thermosyphon was charged for a liquid column height of 39 mm (full fill) from the base of the evaporator chamber (as shown in Fig. 2). After charging, the thermosyphon was evacuated to a pressure of 2.5 kPa. Foam insulation was applied over the evaporator, the condenser, and the tubing before starting the heat input to the system. The desired saturation temperature in the evaporator was maintained by compensating for the heat loss in the evaporator with the help of a thermofoil heater, wrapped around the evaporator chamber. The existence of saturation conditions inside the system was checked with the correspondence between the temperature and pressure measured at a particular point in the loop (Fig. 1). After the saturation temperature was reached in the evaporator, the experiments were started with an initial heat input of 2 W and increasing in steps of 2 W until reaching 10 W; then 10–20 W in steps of 5 W; 20–50 W in steps of 10 W; 50–150 W in steps of 20 W; and beyond 150 W in steps of 10 W to a maximum of 180 W. Around 15–17 runs were performed during boiling at each system pressure, unless CHF was encountered or the highest temperature measured in the copper block reached 140°C. The CHF condition was defined by a temperature rise of 20°C in 20 s of the top-most thermocouple in the heater block. The choice of 140°C was dictated by the structural integrity of the polycarbonate in the heater block housing, parts of which began to melt around 140°C. After reaching the limiting condition, the power input to the system was slowly decreased to 0 V, and the system was allowed to cool down and attain an equilibrium condition with the ambient temperature.

Temperatures were recorded every 3 s throughout the running time of each experimental run. Steady state at a particular heat flux was defined by a variation of less than ±0.3°C of the heater block temperatures about a steady mean value. After the system had reached steady state, the parameters were recorded and the analysis was done with the data recorded in the last 120 s.

Data acquisition consisted of monitoring the temperature and pressure inside the thermosyphon and power input to the heater. The sampling rate for the temperature readings was 300-per-second, per channel, and 900 samples were averaged per channel for one temperature reading. This resulted in one averaged temperature

reading every 3 s per thermocouple. A 20 Hz filter was applied on the channels measuring the AC voltage to optimize the AC measurement accuracy corresponding to the frequency of the supplied voltage. The voltage and current input to the system were measured with the data acquisition system. The current input to the heater was obtained by measuring the voltage drop across a precision resistor ($1 \pm 0.01\ \Omega$) placed in series with the heater. The output from the pressure gauge was in mA, which was converted to absolute pressure using a linear scale for the full range of the gauge output.

IV. Uncertainty Analysis

The thermocouples and the data acquisition system were calibrated with respect to a resistance temperature device (RTD) probe calibration system at five different temperatures (20, 40, 60, 80, and 100°C) to a maximum uncertainty of 0.1°C. Heat flux through the test surface was determined through a combination of electrical and thermal measurements. Eight type T thermocouples were spaced at distances of 7, 9.9, 13, 16, 19.5, 23, 27, and 31 mm from the test surface to measure the temperatures and help in calculating the heat flux through the surface. A numerical two-dimensional heat conduction model considering the copper rod, foam insulation, and the polycarbonate housing showed that the heat flow through the copper rod could be assumed to be linear (axial temperature profiles obtained from the numerical simulation and the linear assumption had a maximum variation in the range of 1–2°C from two test cases). So, the heat flux at the test surface was obtained by calculating the slope of a fitted line through the thermocouple measurements. The power input to the system was obtained by the product of the voltage drop across the cartridge heater and the current flow through the precision resistor. The voltage measurement uncertainty is specified by the manufacturer as 0.045% of the reading. The precision resistor used to measure the current in the circuit was accurate to 1%. The maximum uncertainty in the surface heat flux from electrical power input was ±1.4%. The difference between the heat flux calculated from temperature measurements and the electrical power input was less than 5% at higher heat fluxes (greater than 20 W/cm^2). The measurements at very low heat fluxes (less than 5 W/cm^2) showed a larger scatter (maximum of 20%). The corresponding uncertainty in the wall temperature measurement was about 0.5°C. The vapor pressure in the evaporator was obtained from the National Institute of Standards and Technology (NIST) [30] data, corresponding to the temperature in the vapor zone. The variation in the temperature of the vapor zone was less than 0.5°C, whereas the pressure measured by the transducer showed a variation of less than 10%, based on the theoretically predicted saturation temperature compared with the measured temperature at that location.

V. Results and Discussion

A. Baseline Study

Boiling at subatmospheric pressures was first studied with an emery polished plain copper surface of dimensions 12.7 × 12.7 mm at pressures of 9.7, 15, and 21 kPa, with a full-fill (liquid height = 39 mm) condition. From visual observation, it was found that intermittent bubbles were generating from the surface at long intervals during the initial stages of power input (2–6 W/cm^2), which changed to fully developed boiling at approximately 12 W/cm^2. By that time, the liquid pool was fully agitated from large sized bubbles generating from the plain surface. Beyond 55 W/cm^2, the power input was gradually increased in steps of 3 W/cm^2, until it reached the desired power, at which temperatures were recorded. This was done to closely monitor the point at which CHF was initiated.

Figure 4 shows the resulting boiling curves at the pressures of 9.7, 15, and 21 kPa. Data from McGillis et al. [20] and Latsch et al. [31], as well as the boiling curve of FC-72 (nucleate boiling zone only) derived from the correlation developed by Rainey et al. [21] are also shown for comparison. The improvement in heat transfer obtained with boiling of water with respect to FC-72 is clearly evident. At

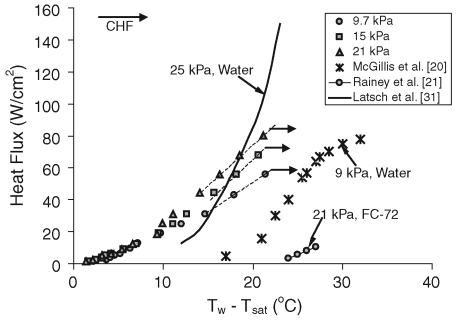

Fig. 4 Boiling curve for water on a plain surface at full-fill level in the evaporator.

80 W/cm^2 the wall superheat for water was around 20°C compared with 55°C for FC-72. Existence of incipient superheat is a common phenomenon in boiling of dielectric liquids (Rainey et al. [21], Anderson and Mudawar [26], Ramaswamy et al. [28]), and is found to depend on the saturation pressure. However, the present study shows that saturation pressure has negligible effect on the incipient superheat in boiling of water. Gebhart and Wright [32,33] noticed a similar absence of incipience in boiling of water with micro-configured surfaces and suggested the existence of early incipience and microboiling from the observations. However, McGillis et al. [20] noticed wall superheats in excess of 5°C in their study on boiling of water from a plain surface of dimensions 12.7 × 12.7 mm (the results at 9 kPa are shown in Fig. 4). They noticed fewer active nucleation sites for boiling with plain surface, which was responsible for higher wall superheats. It is to be noted that the evaporator chamber of McGillis et al. [20] was not insulated. Because of heat loss from the evaporator wall, a large wall superheat was required to reach saturated conditions at 9 kPa. This is markedly different from the present study, in which the heat loss from the evaporator wall was compensated for with a guard heater, which kept the bulk liquid temperature close to the saturation temperature. As a result, the wall superheat was very low during the initial stages of boiling (compared with McGillis et al. [20]).

The effect of pressure is clearly evident, as the heat flux capability is considerably decreased with a reduction in saturation pressure. However, the effect of pressure is not noticed below 20 W/cm^2. Beyond 20 W/cm^2, the boiling curves show linear behavior until CHF is reached. Van Stralen [13] observed a similar decrease in the maximum heat flux with a decrease in pressure, which was attributed to the larger size of bubbles generating from the heating surface. Joudi and James [17] observed a reduction in the number of bubbles generated from the boiling surface at reduced pressures. Fath and Judd [18] observed a similar increase in heat flux with increase in system pressure, though their experiments were with dichloro-methane. Bubble generation frequency increased with increase in pressure. Other studies, which corroborate the preceding observations, are by Tewari et al. [19], Latsch et al. [31] and Gorodov et al. [34]. However, the decrease in the heat flux is offset by the reduction in saturation temperature inside the evaporator chamber with decrease in saturation pressure. This is particularly interesting for electronic cooling applications, as very low surface temperature can be obtained under these conditions. The maximum wall temperatures recorded for the pressures of 9.7, 15, and 21 kPa were 68, 76, and 83°C, respectively.

CHF was reached for all the cases under consideration. For 9.7 kPa, the CHF was 62 W/cm^2, whereas for 15 and 21 kPa it was 78 W/cm^2 and 87 W/cm^2, respectively. However, McGillis et al. [20] obtained a higher CHF (greater than 80 W/cm^2) at 9 kPa from a plain copper surface. As discussed in the preceding paragraphs, the absence of insulation in the evaporator chamber can explain the high CHF obtained with respect to the present study. Because of heat transfer through the evaporator wall, the effective heat transfer coefficient in the evaporator was much higher in their case, which resulted in higher CHF than that observed in the present study. In this respect, it is believed that the current study documents a more

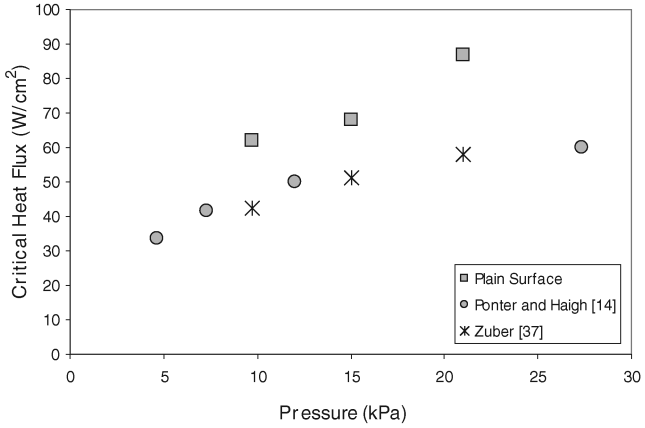

Fig. 5 Comparison of CHF values for boiling with plain surface.

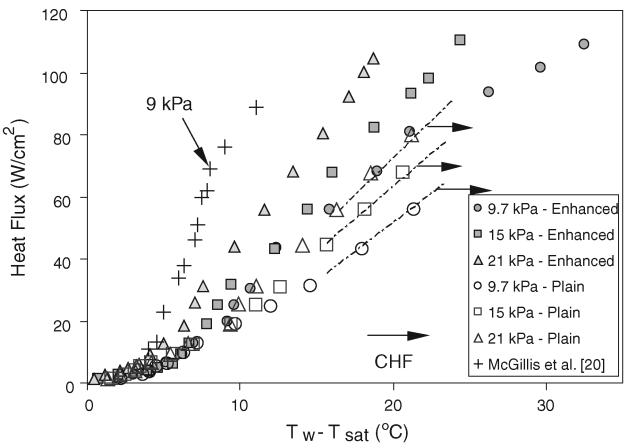

Fig. 6 Effect of pressure on enhanced single-layer structure and plain surface.

controlled investigation of boiling at subatmospheric pressures. A recent study by Pal and Joshi [35] has shown that the CHF can be increased in subatmospheric pressure boiling of water by lowering the effective liquid level in the evaporator. The liquid level in the case of McGillis et al. [20] was much lower than the present study, which might also explain the higher CHF obtained by them.

In Fig. 5 a comparison of the CHF values with respect to existing correlations is shown. The experimental results of Ponter and Haigh [14] match the predictions of the Zuber [37] correlation reasonably well. Ponter and Haigh [14] used a tubular stainless steel heater, which was immersed under 76 mm of liquid column. The present CHF values are higher by a factor in the range of 1.3–1.5 with respect to the preceding observations. As pointed out by Carey [36], Zuber's model [37] did not account for the possible effects of surface condition and wetting characteristics of the heater surface, which might explain the discrepancy in the CHF values with respect to the present results. Moreover, the high liquid column height used by Ponter and Haigh [14] might also lead to lower CHF values, following the observations of Pal and Joshi [35].

With a decrease in the operating pressure, the density of the vapor decreases. As a result, the bubble sizes during boiling at low pressure are larger compared with boiling at atmospheric pressures. Visual observation during degassing showed that the bubbles are dislodged from the surface at a slower rate than boiling from a plain surface at atmospheric pressure. Miyauchi and Yokura [15] observed similar suppressed bubble growth rates at subatmospheric pressures. According to them, a rapidly growing bubble will accelerate the liquid surrounding it, which will induce a pressure increase inside the bubble. It was hypothesized that the increase in pressure will increase the saturation temperature and lead to higher wall superheats, leading to suppressed bubble growth rates. Moreover, the larger size of the bubbles might also inhibit the growth of bubbles from neighboring sites, leading to bubble generation from some preferred sites. This might lead to fluctuations in temperature in the boiling surface. An interesting finding in this respect was by Joudi and James [17], which focused on the surface temperature during the initial boiling stages. They found that the surface temperature was not uniform across the boiling surface or steady at a particular location. In the current experiments, surface temperature fluctuations were not recorded, instead average surface temperatures obtained from the linear fit of the copper block temperature measurements were used to report the boiling data.

B. Effect of Pressure

The present section will describe the study on various enhancement structures at the pressures of 9.7, 15, and 21 kPa and compare the results with the baseline study reported earlier. Four boiling enhancement structures were used, which have different numbers of stacked layers (1, 2, 4, and 6) with geometries as described earlier. The experiments described in this section were done at full-fill level for all the pressures and the different enhancement structure geometries.

In Fig. 6, the effect of pressure on the saturated nucleate boiling curves is compared between the single-layer enhanced structure and the plain surface. The results from McGillis et al. [20] at 9 kPa are also shown for comparison. Both the studies employed the footprint area of the surface enhancement as the base area in obtaining the heat flux. McGillis et al. performed their experiments with finned structures in which the lowest gap between the fins was kept at 0.3 mm. This result is included for comparison, as the fin gap of 0.3 mm closely resembles the gap (0.35 mm) of the channels in the enhancement structure used in the present study. They found better performance with the lowest fin gap. As noticed in case of the plain surface, incipient superheat is not noted for the enhanced structure in the present study. This observation corroborates the results of Gebhart and Wright [32] mentioned earlier. The wall superheat of 4°C at 9 W/cm^2 observed by McGillis et al. [20] agrees roughly with the wall superheat of 6.2°C at 9.3 W/cm^2 observed in the present study. However, a significant difference is noted in the wall superheat at higher heat fluxes. Although CHF was not reached in both of the studies, a difference of approximately 13°C was noted in the wall superheat at around 90 W/cm^2, with McGillis et al. showing the lowest wall superheat. A possible explanation can be the configuration of the thermosyphon used in the two studies. McGillis et al. used a single-chamber thermosyphon, or wickless heat pipe configuration, in which the condenser was placed directly above the evaporator and was an integral part with the evaporator cylinder. This allowed easy draining of the condensed liquid directly to the evaporator. In the present study, a dual-chamber configuration of the thermosyphon was used, in which the condenser tube was inclined with respect to the horizontal. Condensed liquid drained from the condenser only when enough pressure gradient was generated in the condenser. As a result, the condenser was lined with liquid most of the time, which reduced the condensation heat transfer coefficient. Though a vertically oriented condenser will aid in draining the liquid quickly, its added size may be undesirable in compact microsystems.

The nucleate boiling curves for the 2-, 4-, and 6-layer enhancement structures are shown in Figs. 7–9, respectively. Similar to the single-layer case, incipient superheat was absent in the cases of 2-, 4-, and 6-layer structures. Moreover, similar to the single-layer case, an increase in the saturation pressure led to a corresponding increase in the saturation temperature, which was responsible for an increase in the wall temperature. A common trend for all the structures (1, 2, 4, and 6 layers) was that the wall temperature increased at a greater rate for 9.7 kPa, compared with 21 kPa, with an increase in the wall heat flux. This behavior is more apparent at higher heat fluxes (greater than 60 W/cm^2). For the single-layer structure at 9.7 kPa, the wall temperature increased by 15°C (24%) as the heat flux increased from 60 to 100 W/cm^2, whereas the increase was 8°C (12%) and 6°C (8%) for 15 kPa and 21 kPa, respectively. The effect of pressure at a particular heat flux is also apparent. For the single-layer structure at 60 W/cm^2, the wall temperature increased

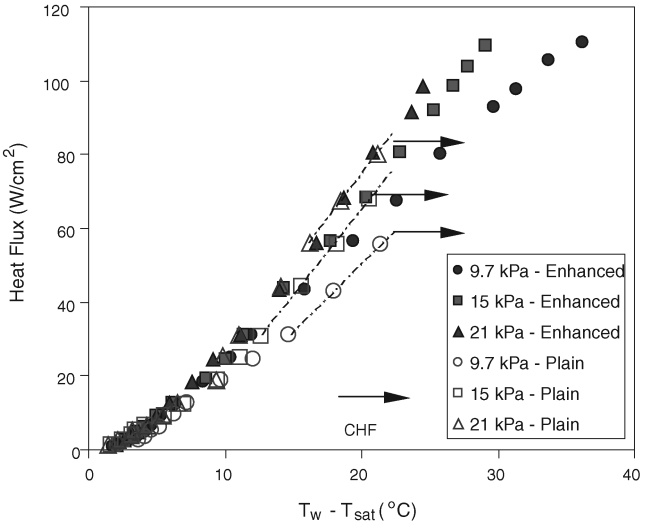

Fig. 7 Effect of pressure on enhanced double-layer structure and plain surface.

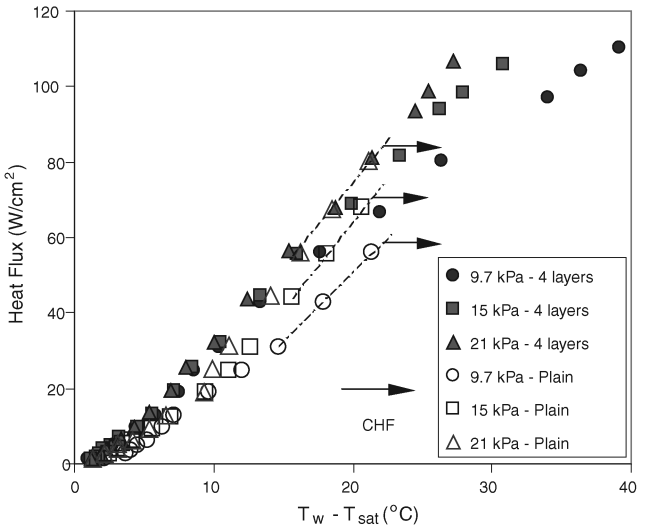

Fig. 8 Effect of pressure on enhanced four-layer structure and plain surface.

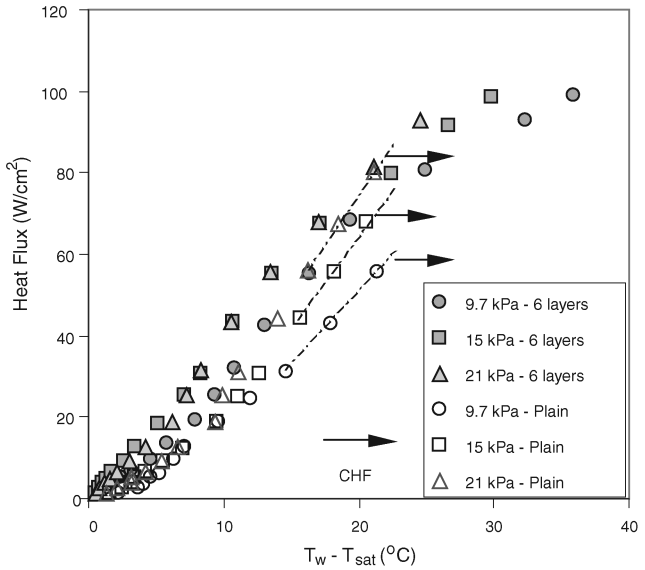

Fig. 9 Effect of pressure on enhanced six-layer structure and plain surface.

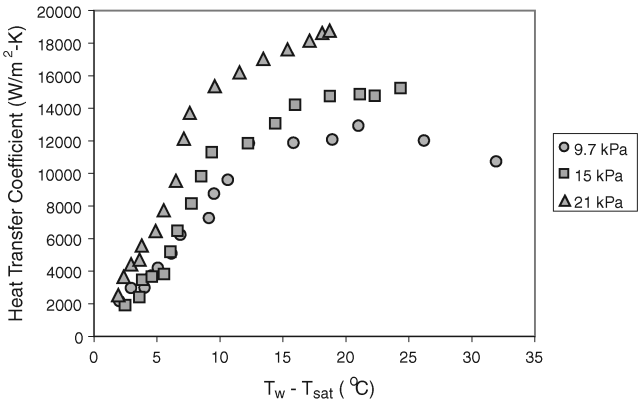

Fig. 10 Heat transfer coefficient as a function of wall superheat for single-layer structure.

by 11°C (24% increase) from 9.7 to 21 kPa. With an increase in heat flux to 80 W/cm^2, the difference dropped slightly to 10°C (15% increase), whereas for 100 W/cm^2, the difference dropped sharply to 4°C (8% increase). This shows that increasing the saturation pressure at a particular heat flux will result in a smaller change of the wall temperature. Similar trends were seen for the other structures too. This behavior can be better understood by observing the variation of the heat transfer coefficient with the wall superheat for a single-layer structure as shown in Fig. 10. A significant trend of a decrease in the heat transfer coefficient with a decrease in pressure is noticed. For 9.7 kPa, the heat transfer coefficient increases monotonically until a wall superheat of 15°C is reached, then slowing until 20°C and reducing beyond that. It is interesting to note the existence of the maximum heat transfer coefficient for the 9.7 kPa and 15 kPa cases. However, the heat transfer coefficient for 21 kPa increases rapidly until 10°C and, subsequently, with a slightly slower rate. The bubble generation process may provide an explanation for worse thermal performance at 9.7 kPa. At lower pressures, the bubble sizes are large, preventing the liquid from coming in contact with the boiling surface and resulting in a decrease in the heat transfer coefficient. The current configuration of the boiling enhancement structure also generates bubbles from the vertical sidewalls, which add to the turbulence in the pool. So the reduction in boiling surface temperatures obtained by operating the thermosyphon at low pressures is offset by the deteriorating heat transfer coefficient.

C. Effect of Enhancement Structure

We can see clearly from Tables 1 and 2, that the enhancement structures were able to dissipate high heat fluxes while keeping surface temperatures very close to the threshold value of 85°C

Table 1 Wall temperatures recorded at 80 W/cm^2

Pressure	1 layer		2 layers		4 layers		6 layers	
(kPa)	T_w	ΔT	T_w	ΔT	T_w	ΔT	T_w	ΔT
9.7	68	21.7	72	25.7	72	25.7	72	25.7
15	73	18	78	23	78	23	78	23
21	78	15.5	84	21.5	84	21.5	84	21.5

[a]$\Delta T = T_w - T_{sat}$, T_w and T_{sat} are in °C.

Table 2 Wall temperatures recorded at 100 W/cm^2

Pressure	1 layer		2 layers		4 layers		6 layers	
(kPa)	T_w	ΔT	T_w	ΔT	T_w	ΔT	T_w	ΔT
9.7	77	30.7	79	32.7	82	35.7	83	36.7
15	77	22	82	27	83	28	85	30
21	81	18.5	87	24.5	89	26.5	90	27.5

[a]$\Delta T = T_w - T_{sat}$, T_w and T_{sat} are in °C.

(desired in electronic cooling applications). However, the performance became worse at 100 W/cm^2 for structures having more than two layers. The CHF was not reached for the enhancement structure geometries until the end of the experimental steps (usually 100 W/cm^2). It is observed that the wall superheat increases with an increase in the number of layers of the structures, which implies a decrease in the heat transfer coefficient. This trend can be seen in Fig. 11, in which the effect of the stack height on the heat transfer coefficient, h, at 9.7 kPa is shown, where

$$h_{\text{ave}} = \frac{Q}{A_s \cdot \Delta T} \tag{1}$$

where Q is the heat dissipation, A_s is the surface area of the structure exposed to liquid, and ΔT is the wall superheat ($T_w - T_{\text{sat}}$). The superior performance of the single-layer structure is evident from the comparison. For the single-layer structure, the heat transfer coefficient increases monotonically at low wall superheat, then slowing down from 10°C–20°C, and finally decreasing monotonically at higher wall superheats. Visual observation showed that at low wall superheats, the bubbles emerged from some preferred spots, however, at higher wall superheats, the bubble generation resembled that of fully developed boiling. The generation of bubbles affected the liquid movement close to the boiling structure. So at higher heat fluxes, vigorous bubble generation decreased the liquid supply close to the structure, which decreased the heat transfer coefficient. Ramaswamy [38] observed similar behavior for boiling with a single-layer structure of similar geometry, using PF5060 as the working fluid. Compared with the single-layer structure, the 2-, 4-, and 6-layer structures show a weaker change in the heat transfer coefficient with wall superheat and achieve lower values of the heat transfer coefficient. An increase in the stack height is also seen to limit the maximum value of the heat transfer coefficient. This implies that there exists a certain stack height, which will produce the maximum heat transfer coefficient for a particular saturation pressure. McGillis et al. [20] also observed similar optimum height with finned structures and found that the heat transfer was insensitive to fin height beyond a certain fin height. In the current study, however, the heat transfer was influenced by the height of the structure. Following from the preceding discussion, this behavior can be attributed to the bubble generation dynamics from the enhancement structure used in the present study.

Increasing the number of layers increases the convection heat transfer area; however, due to the conduction thermal resistance encountered in the stack, the temperature of the top layer will be less than the base temperature, potentially resulting in a decrease in heat transfer coefficient. A similar observation was also noted by Ramaswamy [38] in his study with dielectric fluids. Nakayama et al. [39] noted that for higher heat fluxes (greater than 15 W/cm^2), the boiling curves of porous structures closely resembled that of plain surfaces. They attributed the deterioration in heat transfer coefficient with an increase in the stack height of the porous structures to the "dried-up" mode of boiling. In a recent study with PF5060, Ghiu and Joshi [40] did not observe any decrease in performance due to the dried-up mode, however, the maximum heat flux for their study was 35 W/cm^2. In the present study, experiments were performed beyond 100 W/cm^2, where vigorous bubble generation was observed. Because of increased bubble generation from the sidewalls (with an increasing stack height) and the top surface of the structure, there will be less liquid coming in contact with the porous structure, which would decrease the overall heat transfer from the structure. In this regard, the current results corroborate with the previous observations of Nakayama et al. [39].

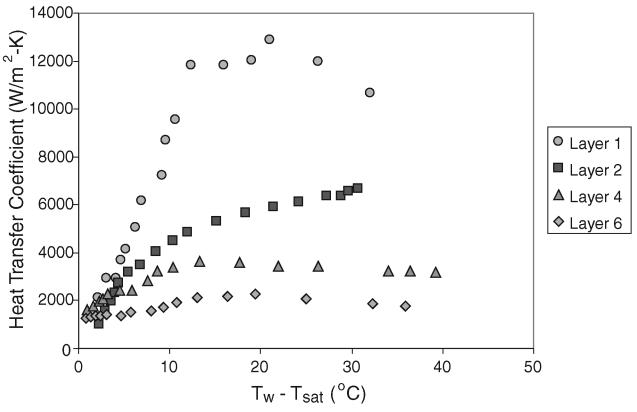

Fig. 11 Heat transfer coefficient vs wall superheat at 9.7 kPa for all layers.

D. Fin Model

The enhanced structure was modeled as a fin with a specified heat transfer coefficient. The following additional assumptions were made:

1) Heat losses from the sides of the chamber were considered negligible.

2) Uniform heat flux was assumed from the heater surface.

3) The heat transfer coefficient was obtained by considering the exposed surface of the structure to be at the wall temperature.

4) The uniform heat transfer coefficient was assumed over the entire exposed surface of the boiling structure.

Three-dimensional steady heat conduction was employed for the configuration shown in Fig. 12, using the following boundary conditions:

Input heat flux:

$$q''_h = \frac{Q}{A} \tag{2}$$

Convective heat transfer:

$$k_c \left.\frac{\partial T}{\partial z}\right|_s = h_{\text{ave}}(T_{\text{sat}} - T_s) \tag{3}$$

where Q is the input power to the system; A is the heater surface area, which was in contact with the copper block; h_{ave} is the average heat transfer coefficient at the exposed surfaces of the enhanced structure (obtained from the experimental results); T_{sat} is the saturation temperature of the working fluid; and T_s is the temperature at the surfaces of the enhanced structure. The solution procedure involved solving for the temperature profile throughout the assembly and then obtaining the heat flux from the base of the structure. The q'' vs T curves for layers 1, 4, and 6 obtained from the numerical simulation are shown in Fig. 13, alongside experimental data. The trends of the predicted q'' vs T curves match closely with those of the experimental results, which shows that the numerical simulation predicted the enhancement obtained from the structures. However, the numerical simulation overpredicted the surface heat flux by approximately 5%

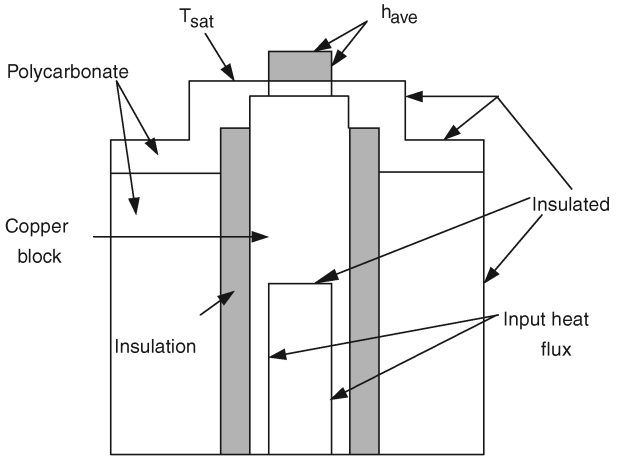

Fig. 12 Model configuration for calculation of wall heat flux with enhanced structures.

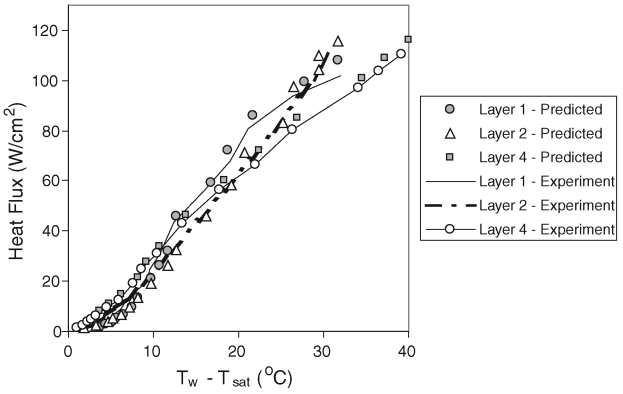

Fig. 13 Effect of varying stack height on boiling heat transfer (comparison between experimental and numerically predicted results).

at the higher heat fluxes. One of the reasons for this overprediction might be the assumption of the uniform heat transfer coefficient throughout the exposed surface of the enhancement structure. Moreover, adiabatic conditions were assumed for all the sidewalls and the bottom walls of the assembled structure shown in Fig. 12. In reality, some heat loss will occur through the sidewalls, which will reduce the actual heat flux through the boiling surface. Ramaswamy [38] performed a two-dimensional analysis of the heat transfer through the enhanced structures using a finite volume approach. Their predicted surface heat flux values had a minimum of 10% variation with respect to their experimental results. A more realistic three-dimensional analysis in this study might be responsible for the better agreement between predicted and experimental results. This study shows that the fin effect of the enhancement structures cannot be neglected. The combined effect of the finlike structures and the boiling phenomenon from stacked porous structures might be responsible for the observed reduction in heat transfer coefficient with an increase in the layers of the enhancement structure.

Increasing the layers of the structures also affects the flowfield inside the evaporator, which might also explain the deterioration of heat transfer for higher stack heights. A tall structure would create a barrier to the flow coming from the inlet. During boiling, such a structure would also generate more bubbles from the sides, which would create both a sweeping motion and resistance to the incoming liquid from coming in contact with the structure. Structures with lower heights would provide smaller resistance to the incoming flow. The top side of the structure would be the main contributor to heat dissipation. Haider et al. [11] performed a numerical study of the flow and heat transfer of a closed-loop thermosyphon and observed that the heat transfer in a thermosyphon configuration as used in the present study would be similar to the heat transfer in flow boiling.

VI. Conclusions

The boiling of water at subatmospheric pressures from an enhanced structure in a thermosyphon was studied. The enhancement structure had a stacked-layer geometry, and four different numbers of layers were used (1, 2, 4, and 6) at pressures of 9.7, 15, and 21 kPa. The results were also compared with boiling from a plain surface. The following conclusions can be drawn from the experimental results:

1) Boiling at subatmospheric pressures results in a lowering of the saturation temperature, which leads to lower wall temperatures. Heat fluxes greater than 100 W/cm^2 can be achieved through boiling at subatmospheric pressures, while keeping the surface temperatures below the threshold temperature of 85°C.

2) Incipient superheat was found to be negligible for boiling at subatmospheric pressures with enhanced structures.

3) The heat transfer coefficient increased with an increase in the operating pressure. With an increase in heat flux, the performance at lower pressure was worse compared with higher pressure.

4) The lowering of surface temperature with a decrease in pressure is offset by the deterioration of heat flux with the lowering of pressure. Bubble generation physics plays an important part in this scenario. In this respect, the current results corroborate previous investigations on boiling of water at low pressures, which concentrated on visualization of bubble generation at low pressures.

5) The enhancement structure is found to increase the heat flux with respect to boiling from a plain surface at subatmospheric pressures. However, as the height of the structure was increased beyond a single layer, the heat transfer coefficient was reduced. This implies the existence of an optimum height of the structure, which will achieve the maximum heat transfer corresponding to a particular saturation pressure.

6) The enhanced structure achieved improved performance with respect to the plain surface and also increased the CHF.

7) With an increase in the operating pressure, the enhancement in heat transfer achieved by the porous structure over the plain surface tends to decrease.

Acknowledgment

The authors acknowledge support for this research work from the National Science Foundation Microsystems Packaging Research Center at the Georgia Institute of Technology.

References

[1] Tengblad, N., and Palm, B., "External Two Phase Thermosiphons for Cooling of Electronic Components," *International Journal of Microcircuits and Electronic Packaging*, Vol. 19, No. 1, 1996, pp. 22–29.

[2] Palm, B., and Tengblad, N., "Cooling of Electronics by Heat Pipes and Thermosyphons—A Review of Methods and Possibilities," *National Heat Transfer Conference*, Vol. 329, Heat Transfer Div., American Society of Mechanical Engineers, New York, 1996, pp. 97–108.

[3] Ramaswamy, C., Joshi, Y., Nakayama, W., and Johnson, W. B., "Performance of a Compact Two-Phase Thermosyphon: Effect of Evaporator Inclination, Liquid Fill Volume and Contact Resistance," *Proceedings of the 11th International Heat Transfer Conference*, Vol. 2, 1998, pp. 127–132.

[4] Ramaswamy, C., Joshi, Y., Nakayama, W., and Johnson, W. B., "Compact Thermosyphons Employing Microfabricated Components," *Microscale Thermophysical Engineering*, Vol. 3, No. 4, 1999, pp. 273–282.
doi:10.1080/108939599199693

[5] Ramaswamy, C., Joshi, Y., Nakayama, W., and Johnson, W. B., "Thermal Performance of a Compact Two-Phase Thermosyphon: Response to Evaporator Confinement and Transient Loads," *Journal of Enhanced Heat Transfer*, Vol. 6, Nos. 2–4, 1999, pp. 279–288.

[6] Ramaswamy, C., Joshi, Y., Nakayama, W., and Johnson, W. B., "Combined Effects of Sub-Cooling and Operating Pressure on the Performance of a Two-Chamber Thermosyphon," *IEEE Transactions on Components and Packaging Technologies*, Vol. 23, No. 1, Mar. 2000, pp. 61–69.
doi:10.1109/6144.833043

[7] Yuan, L., Joshi, Y. K., and Nakayama, W., "Effect of Condenser Location and Imposed Circulation on the Performance of a Compact Two-Phase Thermosyphon," *Nanoscale and Microscale Thermophysical Engineering*, Vol. 7, No. 2, Apr. 2003, pp. 163–179.

[8] Webb, R. L., and Yamauchi, S., "Thermosyphon Concept to Cool Desktop Computers and Servers," *Proceedings of the International Electronic Packaging Technical Conference and Exhibition*, 2001.

[9] Garner, S. D., and Patel, C. D., "Loop Thermosyphons and Their Applications to High Density Electronics Cooling," *Proceedings of the International Electronic Packaging Technical Conference and Exhibition*, 2001.

[10] Yuan, L., Joshi, Y., and Nakayama, W., "Effect of Condenser Location and Tubing Length on the Performance of a Compact Two-Phase Thermosyphon," *Proceedings of 2001 International Mechanical Engineering Congress and Exposition*, American Society of Mechanical Engineers, New York, Nov. 11–16, 2001.

[11] Haider, S. I., Joshi, Y. K., and Nakayama, W., "A Natural Circulation Model of the Closed Loop, Two-Phase Thermosyphon for Electronics Cooling," *Journal of Heat Transfer*, Vol. 124, No. 5, 2002, pp. 881–890.
doi:10.1115/1.1482404

[12] Pal, A., Joshi, Y., Beitelmal, M. H., Patel, C. D., and Wenger, T., "Design and Performance Evaluation of a Compact Thermosyphon,"

IEEE Transactions on Components and Packaging Technologies, Vol. 25, No. 4, 2002, pp. 601–607. doi:10.1109/TCAPT.2002.807997

[13] Van Stralen, S. J. D., "Heat Transfer to Boiling Binary Liquid Mixtures at Atmospheric and Subatmospheric Pressures," *Chemical Engineering Science*, Vol. 5, No. 6, Feb. 1956, pp. 290–296. doi:10.1016/0009-2509(56)80004-3

[14] Ponter, A. B., and Haigh, C. P., "The Boiling Crisis in Saturated and Subcooled Pool Boiling at Reduced Pressures," *International Journal of Heat and Mass Transfer*, Vol. 12, No. 4, Apr. 1969, pp. 429–437. doi:10.1016/0017-9310(69)90138-0

[15] Miyauchi, T., and Yokura, M., "The Mechanism of Nucleate Boiling Heat Transfer," *Heat Transfer - Japanese Research*, Vol. 1, No. 2, 1972, pp. 109–118.

[16] Van Stralen, S. J. D., Cole, R., Sluyter, W. M., and Sohal, M. S., "Bubble Growth Rates in Nucleate Boiling of Water at Subatmospheric Pressures," *International Journal of Heat and Mass Transfer*, Vol. 18, No. 5, May 1975, pp. 655–669. doi:10.1016/0017-9310(75)90277-X

[17] Joudi, K. A., and James, D. D., "Incipient Boiling Characteristics at Atmospheric and Subatmospheric Pressures," *Journal of Heat Transfer*, Vol. 99, No. 3, 1977, pp. 398–403.

[18] Fath, H. S., and Judd, R. L., "Influence of System Pressure on Microlayer Evaporation Heat Transfer," *Journal of Heat Transfer*, Vol. 100, 1978, pp. 49–55.

[19] Tewari, P. K., Verma, R. K., Ramani, M. P. S., Chatterjee, A., and Mahajan, S. P., "Nucleate Boiling in a Thin Film on a Horizontal Tube at Atmospheric and Subatmospheric Pressures," *International Journal of Heat and Mass Transfer*, Vol. 32, No. 4, 1989, pp. 723–728. doi:10.1016/0017-9310(89)90219-6

[20] McGillis, W. R., Carey, V. P., Fitch, J. S., and Hamburgen, W. R., "Pool Boiling Enhancement Techniques for Water at Low Pressure," *Proceedings of the Seventh IEEE SEMI-THERM Symposium*, 1991, pp. 64–72.

[21] Rainey, K. N., You, S. M., and Lee, S., "Effect of Pressure, Subcooling and Dissolved Gas on Pool Boiling Heat Transfer from Microporous Surfaces in FC-72," *Journal of Heat Transfer*, Vol. 125, No. 1, 2003, pp. 75–83. doi:10.1115/1.1527890

[22] Nakayama, W., Daikoku, T., Kuwahara, H., and Nakajima, T., "Dynamic Model of Enhanced Boiling Heat Transfer on Porous Surfaces, Part I: Experimental Investigation," *Journal of Heat Transfer*, Vol. 102, 1980, pp. 445–450.

[23] Bergles, A. E., and Chyu, M. C., "Characteristics of Nucleate Pool Boiling from Porous Metallic Coatings," *Journal of Heat Transfer*, Vol. 104, No. 5, 1982, pp. 279–285.

[24] Marto, P. J., and Lepere, V. J., "Pool Boiling Heat Transfer from Enhanced Surfaces to Dielectric Fluids," *Journal of Heat Transfer*, Vol. 104, 1982, pp. 292–299.

[25] Nakayama, W., Nakajima, T., and Hirasawa, S., "Heat Sink Studs Having Enhanced Boiling Surfaces for Cooling of Microelectronic Components," American Society of Mechanical Engineers Paper 84-WA/HT-89, 1984.

[26] Anderson, T. M., and Mudawar, I., "Microelectronic Cooling by Enhanced Pool Boiling of a Dielectric Fluorocarbon Liquid," *Journal of Heat Transfer*, Vol. 111, 1989, pp. 752–759.

[27] Pal, A., and Joshi, Y., "Boiling at Sub-Atmospheric Conditions with Enhanced Structures," *The Tenth Intersociety Conference on Thermal and Thermomechanical Phenomena in Electronics Systems*, 2006.

[28] Ramaswamy, C., Joshi, Y., Nakayama, W., and Johnson, W. B., "Effects of Varying Geometrical Parameters on Boiling from Microfabricated Enhanced Structures," *Journal of Heat Transfer*, Vol. 125, 2003, pp. 103–109. doi:10.1115/1.1513575

[29] Launay, S., Federov, A., Joshi, Y., Cao, A., and Ajayan, P. M., "Hybrid Micro-Nano Structured Thermal Interfaces for Pool Boiling Heat Transfer Enhancement," *Proceedings of THERMINIC 2004*, 2004, pp. 299–304.

[30] Anon., "NIST Chemistry WebBook," *NIST Standard Reference Database No. 69* [online database], http://webbook.nist.gov/chemistry/ [retrieved 15 Aug. 2008].

[31] Latsch, K., Morell, F., and Rampf, H., "Subcooled Forced Convection Boiling Heat Transfer at Subatmospheric Pressure," *Proceedings of the Sixth International Heat Transfer Conference*, 1978, pp. 287–292.

[32] Gebhart, B., and Wright, N., "Boiling Enhancement of Micro-configured Surfaces," *International Communications in Heat and Mass Transfer*, Vol. 15, 1988, pp. 141–149. doi:10.1016/0735-1933(88)90061-9

[33] Wright, N., and Gebhart, B., "Enhanced Boiling on Microconfigured Surfaces," *Journal of Electronic Packaging*, Vol. 111, 1989, pp. 112–120.

[34] Gorodov, A. K., Kaban'kov, O. N., Komov, A. T., and Yagov, V. V., "Critical Boiling Heat Fluxes to Liquids at Subatmospheric Pressures," *Heat Transfer: Soviet Research*, Vol. 11, No. 3, May–June 1979, pp. 53–61.

[35] Pal, A., and Joshi, Y., "Boiling of Water at Subatmospheric Conditions with Enhanced Structures—Effect of Liquid Fill Volume," *Journal of Electronic Packaging*, Vol. 130, No. 1, Mar. 2008, Paper 011010.

[36] Carey, V. P., "Pool Boiling," *Liquid-Vapor Phase Change Phenomenon*, Hemisphere, New York, Feb. 1992, p. 250.

[37] Zuber, N., "Hydrodynamic Aspects of Boiling Heat Transfer," *Physics and Mathematics*, AEC, Rept. AUCU-4439, 1959.

[38] Ramaswamy, C., "A Compact Two-Phase Thermosyphon Employing Microfabricated Boiling Enhancement Structures," Ph.D. Dissertation, Univ. of Maryland, College Park, MD, 1999.

[39] Nakayama, W., Daikoku, T., and Nakajima, T., "Effects of Pore Diameter and System Pressure on Saturated Pool Nucleate Boiling Heat Transfer from Porous Surfaces," *Journal of Heat Transfer*, Vol. 104, 1982, pp. 286–291.

[40] Ghiu, C. D., and Joshi, Y., "Boiling Performance of Single-Layered Enhanced Structures," *Journal of Heat Transfer*, Vol. 127, No. 7, 2005, pp. 675–683. doi:10.1115/1.1924568